Inorganic Chemistry

pubs.acs.org/IC Communication

Mechanochemical Access to Catechol-Derived Metal—Organic Frameworks

Fillipp Edvard Salvador, Jesus O. Barajas, and Wen-Yang Gao*



Cite This: Inorg. Chem. 2023, 62, 3333-3337



ACCESS I

III Metrics & More

Article Recommendations



ABSTRACT: Mechanochemistry, a resurging synthetic approach, has been developed into an effective and controllable method to access a family of crystalline porous catechol-derived metal—organic frameworks (MOFs) for the first time. We have identified that the obtained crystalline phase is readily tunable by precursors and the addition of solvents or drying agents. The described mechanochemistry allows us to synthesize these materials in a highly sustainable manner. Thus, mechanochemistry is expected to pave a promising avenue to access a broader class of MOF materials, in addition to those based on the motifs of carboxylic acid or imidazole.

atechol-derived metal-organic frameworks (MOFs), a subfamily of MOFs built by the self-assembly of metal ions and hydroxyquinone- or catechol-based ligands, have recently garnered significant attention as a unique class of functional porous materials. 1-5 In particular, the noninnocence brought by ligand-based redox-active behavior results in attractive coordination materials with potential applications in areas of magnetism, ⁶⁻⁹ conductivity, ¹⁰⁻¹⁴ and energy conversion and storage. ^{2,15,16} Meanwhile, mechanochemistry is a resurging synthetic method that drives chemical reactions via mechanical forces instead of heat, light, or electricity, avoids high temperature and solvents, and offers a remarkably sustainable alternative to conventional synthetic routes. 17-2 With regard to the synthesis of MOFs, mechanochemistry has demonstrated its applicability to the synthesis of classic structures (e.g., HKUST-1, MOF-5, MOF-74, ZIFs, UiOs series)²³⁻³¹ that only involve linkage motifs of carboxylic acid or imidazole. Catechol-derived MOFs have not yet been accessed by the mechanochemical synthesis.

Herein, we report our systematic efforts in developing mechanochemistry as an effective and controllable synthetic strategy to easily access a family of catechol-derived MOFs. For instance, known procedures to access an example of these MOFs, $[M_2(dhbq)_3](Bu_4N)_2$ $(H_2dhbq = 2.5-dihydroxy-1.4$ benzoquinone), are described by either the in situ hydrolysis of 2,5-diamino-1,4-benzoquinone (dabq) at high temperature for an extended period of time³² or the slow addition of $M(OAc)_2$ (M = Ni and Co) to the solution of H_2 dhbq under an inert atmosphere (Figure 1a,b).33 This work presents a new synthetic pathway, mechanochemistry, that enables access to $[M_2(dhbq)_3](Bu_4N)_2$ (M = Zn and Cu) in a green and controllable manner (Figure 1c). The developed mechanochemical synthesis is accomplished by one-pot loading in air under solvent-free conditions at ambient temperature for a short period of time, which underlines features of sustainability and environmental friendliness. Beyond the doubly interpenetrated three-dimensional (3D) [M₂(dhbq)₃](Bu₄N)₂, the mechanochemistry is immediately extended to a series of catechol-derived MOFs based on other ligands, as shown in Figure 1d.

The 3D $[M_2(dhbq)_3](Bu_4N)_2$ structure (Figure 2a,b), initially reported by Abrahams et al.,³² features a (10,3)-a topology network with octahedral M(II) centers bridged by three dhbq anions and tetrabutylammonium (Bu₄N⁺) as the countercation. Aiming at $[Zn_2(dhbq)_3](Bu_4N)_2$, we initiated our investigation by milling anhydrous zinc sulfate (ZnSO₄), H₂dhbq, and tetrabutylammonium bromide [TBAB or (Bu₄N)Br] without any additive solvent at 30 Hz for 1 h. Powder X-ray diffraction (PXRD) analysis of the obtained solids (blue line in Figure 3) indicates a mixture of the targeted 3D structure and the one-dimensional (1D) linear chain of [Zn(dhbq)(OH₂)₂] (indicated by 2θ at 12.2°, 26.1°, and 28.4° labeled by dashed lines in Figure 3). As shown in Figure 2c, the linear chain is composed of alternating Zn(II) cations and dhbq anions, isostructural to $[M(dhbq)(OH_2)_2]$ (M = Mn and Co). 34,35 Each dhbq anion acts as a bridging linker coordinating to two Zn(II) ions on the equatorial plane in a trans arrangement. Hexacoordination of the Zn(II) cation is completed by two aqua ligands occupying axial positions. The pure phase of the 1D [Zn(dhbq)(OH₂)₂], illustrated by PXRD patterns in Figure 3 (green line), is immediately accessible by milling only H₂dhbq and ZnSO₄ under neat conditions without Na₂SO₄ or TBAB.

In order to obtain the pure 3D phase, we have identified that the addition of an appropriate amount of water scavengers, such as sodium sulfate (Na₂SO₄), allows us to effectively prevent the formation of 1D chains and access the desired 3D structure (red line in Figure 3; see more details in Figure S1–

Received: November 16, 2022 Published: February 15, 2023





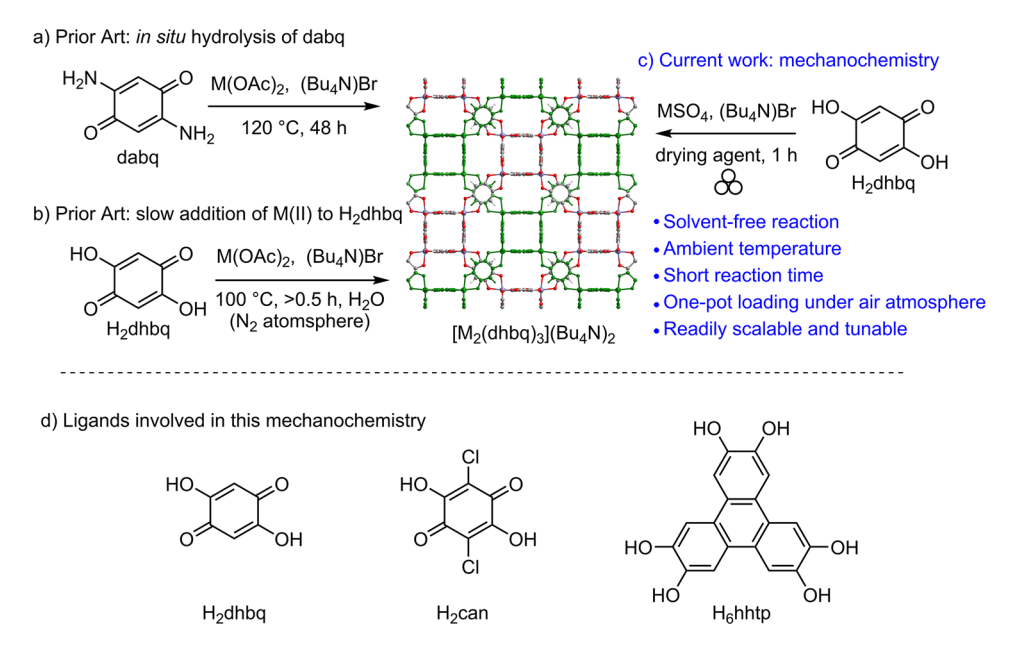


Figure 1. (a and b) Prior art to access $[M_2(dhbq)_3](Bu_4N)_2$, an example of 3D doubly interpenetrated MOFs, available by either *in situ* hydrolysis of dabq at high temperature for an extended period of time or the slow addition of $M(OAc)_2$ (M = Ni and Co) to the solution of H_2dhbq under an inert atmosphere. (c) New synthetic pathway, mechanochemistry, that allows us to access $[M_2(dhbq)_3](Bu_4N)_2$ (M = Zn and Cu) in a green and controllable manner. (d) Described mechanochemistry that is readily generalizable to other ligands, including H_2 can and H_6 hhtp.

S4). The presence of Na₂SO₄ and its amount in the reaction are crucial to afford the 3D phase, which is highlighted by control experiments: (1) As mentioned, milling H₂dhbq, ZnSO₄, and TBAB without Na₂SO₄ generates mixed phases; (2) Milling H₂dhbq, ZnSO₄, and TBAB with the addition of *N,N*-dimethylformamide ($\eta = 0.05 \mu L/mg$) or H₂O ($\eta =$ $0.05-0.8 \mu L/mg$) also provides mixed phases (Figure S1), while increasing the amount of H₂O makes peaks of the 1D chain intensify. (3) A total of 1.9 equiv of Na₂SO₄ (relative to the stoichiometry of ZnSO₄) guarantees formation of the pure 3D phase because 1.0 equiv of Na₂SO₄ still gives mixed phases (Figure S2). The initially introduced Na₂SO₄ was cleaned up by postsynthetic water washing to afford the expected pure 3D structure further verified by the elemental analysis results (see details in the Supporting Information, SI). Additional attempts to replace Bu₄N⁺ with smaller countercations (e.g., tetraethylammonium, Et₄N⁺) by employing (Et₄N)Br, instead of (Bu₄N)Br, only afford the 1D chain of [Zn(dhbq)(OH₂)₂] rather than the 3D network (Figure S2). Employing zinc acetate dihydrate [Zn(OAc)₂·2H₂O] for mechanochemical synthesis with H₂dhbq and TBAB cannot produce the pure 3D phase under various conditions (Figure S4a), possibly due to the presence of water in the zinc precursor.

The completeness of the mechanochemical reactions to access $[Zn_2(dhbq)_3](Bu_4N)_2$ and $[Zn(dhbq)(OH_2)_2]$ is monitored through infrared (IR) spectroscopy by examining the disappearance of the O–H stretch at $3300~cm^{-1}$ and the noncoordinated carbonyl stretch at $1616~cm^{-1}$ along with the shift of the C–O stretch at $1120~cm^{-1}$ observed in the free ligand (Figure S5). The chelated carbonyl group displays a stretching vibration at $1508~cm^{-1}$ in the 3D $[Zn_2(dhbq)_3]$ -(Bu_4N)_2 and at $1537~cm^{-1}$ in the 1D $[Zn(dhbq)-(OH_2)_2]$. 16,35,36 Other characterization data, including UV–vis diffuse-reflectance spectra (Figure S6), thermogravimetric analysis (TGA) plots (Figure S7), and N2 adsorption isotherms at 77 K (Figure S8), were collected on the samples

of $[Zn_2(dhbq)_3](Bu_4N)_2$ and $[Zn(dhbq)(OH_2)_2]$. The TGA plot of $[Zn_2(dhbq)_3](Bu_4N)_2$ indicates that no weight loss is observed before 305 °C, the same as the thermal behavior of the sample prepared by the hydrolysis of dabq. The Brunauer-Emmett-Teller (BET) surface area of $[Zn_2(dhbq)_3](Bu_4N)_2$ is calculated as 41 m²/g (P/P_0 = 0.02–0.15) based on N_2 adsorption isotherms at 77 K. The low surface area is comparable to the surface area of its isostructure, attributed to the countercation of Bu_4N^+ occupying the pore cavities. The same area of the surface area of the process of the surface area of

Moreover, the developed mechanochemical synthesis allows us to prepare an isostructural 3D network, [Cu₂(dhbq)₃]- $(Bu_4N)_2$, under similar reaction conditions. We have identified that the milling of CuSO₄, H₂dhbq, and (Bu₄N)Br requires the addition of 4.2 equiv of MgSO₄ (relative to the stoichiometry of CuSO₄) to the reaction to access the pure phase of $[Cu_2(dhbq)_3](Bu_4N)_2$ (see more details in the SI). The mechanochemically synthesized [Cu₂(dhbq)₃](Bu₄N)₂ was fully characterized by PXRD (Figure S9), IR (Figure S10), UV-vis (Figure S11), TGA (Figure S12), and N₂ adsorption analysis (Figure S13), which are consistent with observations in the literature.³⁵ The multimetallic materials of $[Zn_mCu_n(dhbq)_3](Bu_4N)_2$ become immediately accessible by loading variable amounts of ZnSO₄ and CuSO₄ to the milling reaction given the solid-state synthesis nature of mechanochemistry. We have explored the synthesis of $[Zn_mCu_n(dhbq)_3](Bu_4N)_2 (m/n = 3/1, 1/1, 1/3, m + n =$ 2), and these materials were characterized by UV-vis spectroscopy (Figure S11), PXRD (Figure S14), IR (Figure S15), and TGA (Figure S16). The TGA plots indicate that multimetallic MOFs demonstrate thermal stability (stable up to 305 °C) similar to that of the single-metal MOFs (Figures S7 and S12). Because the single-metal [Cu₂(dhbq)₃](Bu₄N)₂ shows a broad absorbance across the range of 200-700 nm, the absorbances at 259, 348, and 408 nm [troughs observed in $[Zn_2(dhbq)_3](Bu_4N)_2$ are gradually increased with increasing

Inorganic Chemistry pubs.acs.org/IC Communication

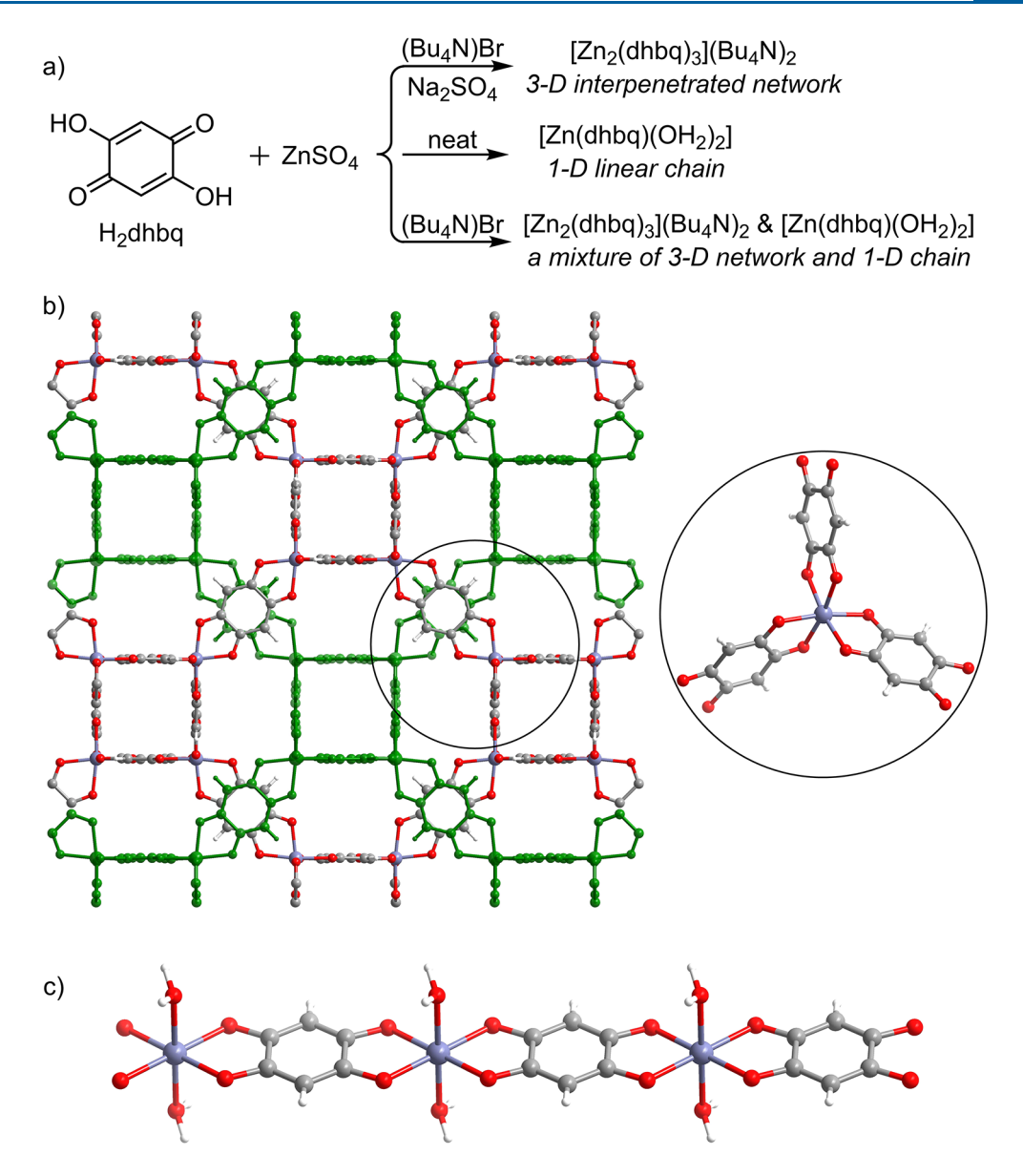


Figure 2. (a) Ball milling of H_2 dhbq and $ZnSO_4$ affording two coordination polymers, which are readily tunable by the additives in the reaction medium. (b) Employment of water scavengers, e.g., Na_2SO_4 , in the presence of TBAB leading to formation of the targeted 3D doubly interpenetrated network. (c) Neat condition without TBAB or Na_2SO_4 generating a 1D linear chain structure. The reaction condition only with TBAB results in a mixture of the 3D network and 1D linear structure.

Cu content in the multimetallic materials (Figure S11). The metal ratios of the resultant materials are confirmed by inductively coupled plasma mass spectrometry (ICP-MS) of samples digested with nitric acid (see details in the SI) and are comparable to the initial reaction loadings.

The developed mechanochemistry is generalized to other types of catechol-derived linkers, including chloranilic acid (H_2 can) and hexahydroxytriphenylene (H_6 hhtp). A family of 3D networks with the formula of [M_2 (can) $_3$](Bu_4N) $_2$) (M=Mn, Zn, or Cd) are obtained by ball milling metal acetate, H_2 can, and (Bu_4N)Br in the presence of methanol (see optimization details in the SI and full characterizations in Figures S17–S25). PXRD analysis (Figure 4) illustrates that these resultant MOFs are isostructural to the reported [Mn_2 (can) $_3$](Bu_4N) $_2$) prepared by the diffusion method using 1,2,4,5-tetrahydroxy-3,6-dichlorobenzene. IR spectra (Figure S19) of [M_2 (can) $_3$](Bu_4N) $_2$) display typical C-H

stretching from the Bu₄N⁺ counterion in the range of 2970-2870 cm⁻¹ and the same vibrational bands with similar shape and intensity between 1800 and 700 cm⁻¹, which suggest the same coordination geometry and the same chemical environment for Mn(II), Zn(II), and Cd(II) complexes.³⁷ These $[M_2(can)_3](Bu_4N)_2$) materials share similar thermal stabilities up to ~310 °C based on TGA (Figure S21) and BET surface areas of 20-40 m²/g derived from N₂ adsorption isotherms at 77 K (Figure S22 and Table S5), which are similar to those of $[M_2(dhbq)_3](Bu_4N)_2$ (M = Zn or Cu). In addition, mechanochemistry allows us to synthesize $[Cu_3(hhtp)_2(OH_2)_6]$, one of the classical metal catecholate frameworks, ³⁸ by milling Cu(OAc)₂·H₂O and H₆hhtp with the addition of H₂O ($\eta = 0.60 \mu L/mg$) for 1 h (see details in the SI and Figures S26-S32). Its phase purity is confirmed by PXRD patterns, which match those of the hydrothermally prepared sample (Figure S26). Significant attenuation of the

Inorganic Chemistry pubs.acs.org/IC Communication

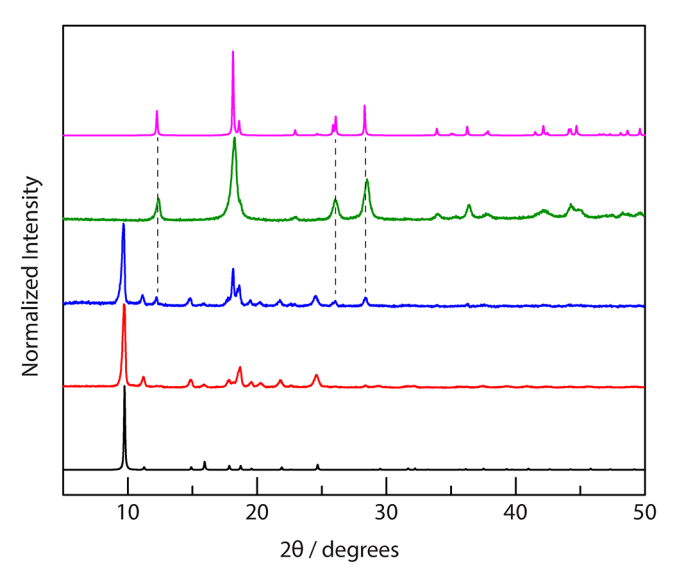


Figure 3. PXRD patterns of the calculated 3D network (black line), the experimentally pure 3D MOF obtained by adding both TBAB and Na_2SO_4 (red line), the mixture of 3D network and 1D chain only in the presence of TBAB (blue line), the experimental 1D chain structure resulting from the neat condition (green line), and the calculated 1D linear coordination polymer (pink line).

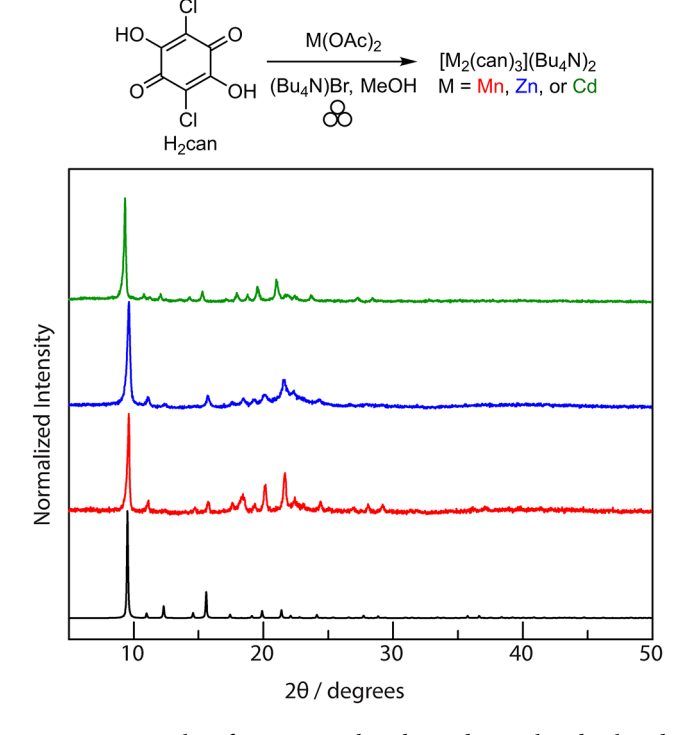


Figure 4. Family of 3D networks obtained via the developed mechanochemical synthesis. PXRD patterns of the calculated network (black line), the as-synthesized Mn-based network (red line), the assynthesized Zn-based network (blue line), and the as-synthesized Cd-based network (green line).

O–H stretch around 3425 cm $^{-1}$ is observed in the IR spectrum of $[Cu_3(hhtp)_2(OH_2)_6]$, along with shifts of C–O stretching at 1225 cm $^{-1}$ and C–O bending at 1145 cm $^{-1}$ initially observed in the linker (Figure S30).

In conclusion, we report a new synthetic strategy, mechanochemical synthesis, to access catechol-derived

MOFs, a distinctive family of MOFs. The mechanochemistry is completed in a highly sustainable manner, which only requires ambient temperature and a short period of reaction time with no or minimal additive solvent. We have identified that the obtained phase is readily tunable by precursors and the addition of solvents or drying agents. The resurging mechanochemistry is expected to pave a promising avenue to access a broader class of MOF materials, in addition to those based on the motifs of carboxylic acid or imidazole.

ASSOCIATED CONTENT

Solution Supporting Information

The Supporting Information is available free of charge at https://pubs.acs.org/doi/10.1021/acs.inorgchem.2c04019.

General considerations, synthesis and characterization, and supporting data, including PXRD patterns, IR spectra, UV-vis diffuse-reflectance spectra, elemental analysis results, TGA plots, ICP-MS data, and N_2 adsorption isotherms (PDF)

AUTHOR INFORMATION

Corresponding Author

Wen-Yang Gao — Department of Chemistry, New Mexico Institute of Mining and Technology, Socorro, New Mexico 87801, United States; ⊚ orcid.org/0000-0002-9879-1634; Email: wenyang.gao@nmt.edu

Authors

Fillipp Edvard Salvador — Department of Chemistry, New Mexico Institute of Mining and Technology, Socorro, New Mexico 87801, United States

Jesus O. Barajas — Department of Chemistry, New Mexico Institute of Mining and Technology, Socorro, New Mexico 87801, United States

Complete contact information is available at: https://pubs.acs.org/10.1021/acs.inorgchem.2c04019

Notes

The authors declare no competing financial interest.

ACKNOWLEDGMENTS

This material is based upon work supported by the National Science Foundation under Grant No. [2213401]. Exploratory studies of the mechanochemistry were supported by the start-up fund of New Mexico Institute of Mining and Technology. We thank Milton Das and Gayan Rubasinghege for the ICP-MS analysis.

REFERENCES

- (1) Darago, L. E.; Aubrey, M. L.; Yu, C. J.; Gonzalez, M. I.; Long, J. R. Electronic Conductivity, Ferrimagnetic Ordering, and Reductive Insertion Mediated by Organic Mixed-Valence in a Ferric Semi-quinoid Metal—Organic Framework. *J. Am. Chem. Soc.* **2015**, *137* (50), 15703—15711.
- (2) Liu, J.; Zhou, Y.; Xie, Z.; Li, Y.; Liu, Y.; Sun, J.; Ma, Y.; Terasaki, O.; Chen, L. Conjugated Copper—Catecholate Framework Electrodes for Efficient Energy Storage. *Angew. Chem., Int. Ed.* **2020**, *59* (3), 1081–1086.
- (3) Cao, J.; Ma, W.; Lyu, K.; Zhuang, L.; Cong, H.; Deng, H. Twist and sliding dynamics between interpenetrated frames in Ti-MOF revealing high proton conductivity. *Chem. Sci.* **2020**, *11*, 3978–3985.

(4) Matheu, R.; Gutierrez-Puebla, E.; Monge, M. Á.; Diercks, C. S.; Kang, J.; Prévot, M. S.; Pei, X.; Hanikel, N.; Zhang, B.; Yang, P.;

- Yaghi, O. M. Three-Dimensional Phthalocyanine Metal-Catecholates for High Electrochemical Carbon Dioxide Reduction. *J. Am. Chem. Soc.* **2019**, *141* (43), 17081–17085.
- (5) Li, L.; Guo, L.; Olson, D. H.; Xian, S.; Zhang, Z.; Yang, Q.; Wu, K.; Yang, Y.; Bao, Z.; Ren, Q.; Li, J. Discrimination of xylene isomers in a stacked coordination polymer. *Science* **2022**, *377* (6603), 335–339.
- (6) Thorarinsdottir, A. E.; Harris, T. D. Metal—Organic Framework Magnets. Chem. Rev. 2020, 120 (16), 8716—8789.
- (7) Mizuno, A.; Shuku, Y.; Awaga, K. Recent Developments in Molecular Spin Gyroid Research. *Bull. Chem. Soc. Jpn.* **2019**, 92 (6), 1068–1093.
- (8) DeGayner, J. A.; Jeon, I. R.; Sun, L.; Dincă, M.; Harris, T. D. 2D Conductive Iron-Quinoid Magnets Ordering up to $T_{\rm c}=105~{\rm K}$ via Heterogenous Redox Chemistry. *J. Am. Chem. Soc.* **2017**, *139* (11), 4175–4184.
- (9) Jeon, I.-R.; Negru, B.; Van Duyne, R. P.; Harris, T. D. A 2D Semiquinone Radical-Containing Microporous Magnet with Solvent-Induced Switching from T_c = 26 to 80 K. *J. Am. Chem. Soc.* **2015**, 137 (50), 15699–15702.
- (10) Xie, L. S.; Skorupskii, G.; Dincă, M. Electrically Conductive Metal-Organic Frameworks. *Chem. Rev.* **2020**, *120* (16), 8536–8560.
- (11) Murase, R.; Leong, C. F.; D'Alessandro, D. M. Mixed Valency as a Strategy for Achieving Charge Delocalization in Semiconducting and Conducting Framework Materials. *Inorg. Chem.* **2017**, *56* (23), 14373–14382.
- (12) Mercuri, M. L.; Congiu, F.; Concas, G.; Sahadevan, S. A. Recent Advances on Anilato-Based Molecular Materials with Magnetic and/or Conducting Properties. *Magnetochemistry* **2017**, 3 (2), 17.
- (13) Monni, N.; Oggianu, M.; Ashoka Sahadevan, S.; Mercuri, M. L. Redox Activity as a Powerful Strategy to Tune Magnetic and/or Conducting Properties in Benzoquinone-Based Metal-Organic Frameworks. *Magnetochemistry* **2021**, *7* (8), 109.
- (14) Skorupskii, G.; Dincă, M. Electrical Conductivity in a Porous, Cubic Rare-Earth Catecholate. *J. Am. Chem. Soc.* **2020**, *142* (15), 6920–6924.
- (15) Calbo, J.; Golomb, M. J.; Walsh, A. Redox-active metal—organic frameworks for energy conversion and storage. *J. Mater. Chem. A* **2019**, *7*, 16571–16597.
- (16) Cai, T.; Hu, Z.; Gao, Y.; Li, G.; Song, Z. A Rationally Designed Iron—Dihydroxybenzoquinone Metal—Organic Framework as Practical Cathode Material for Rechargeable Batteries. *Energy Storage Mater.* **2022**, *50*, 426–434.
- (17) Howard, J. L.; Cao, Q.; Browne, D. L. Mechanochemistry as an emerging tool for molecular synthesis: what can it offer? *Chem. Sci.* **2018**, *9*, 3080–3094.
- (18) Friščić, T.; Mottillo, C.; Titi, H. M. Mechanochemistry for Synthesis. *Angew. Chem., Int. Ed.* **2020**, *59* (3), 1018–1029.
- (19) Szczęśniak, B.; Borysiuk, S.; Choma, J.; Jaroniec, M. Mechanochemical synthesis of highly porous materials. *Mater. Horiz.* **2020**, *7*, 1457–1473.
- (20) Gilman, J. J. Mechanochemistry. Science 1996, 274 (5284), 65.
- (21) Fernández-Bertran, J. F. Mechanochemistry: an overview. *Pure Appl. Chem.* **1999**, 71 (4), 581–586.
- (22) White, S. L.; Heinz, M. W.; Humphrey, S. M. Methods and Diversity in the Synthesis of Metal-Organic Frameworks. In *Comprehensive Coordination Chemistry III*, 3rd ed.; Elsevier, 2021; pp 976–1020. DOI: 10.1016/B978-0-08-102688-5.00086-6.
- (23) Salvador, F. E.; Miller, V.; Shimada, K.; Wang, C.-H.; Wright, J.; Das, M.; Chen, Y.-P.; Chen, Y.-S.; Sheehan, C.; Xu, W.; Rubasinghege, G.; Gao, W.-Y. Mechanochemistry of Group 4 Element-Based Metal—Organic Frameworks. *Inorg. Chem.* **2021**, *60* (21), 16079—16084.
- (24) Klimakow, M.; Klobes, P.; Rademann, K.; Emmerling, F. Characterization of mechanochemically synthesized MOFs. *Microporous Mesoporous Mater.* **2012**, *154* (15), 113–118.
- (25) Lv, D.; Chen, Y.; Li, Y.; Shi, R.; Wu, H.; Sun, X.; Xiao, J.; Xi, H.; Xia, Q.; Li, Z. Efficient Mechanochemical Synthesis of MOF-5 for

- Linear Alkanes Adsorption. J. Chem. Eng. Data 2017, 62 (7), 2030–2036.
- (26) Beldon, P. J.; Fábián, L.; Stein, R. S.; Thirumurugan, A.; Cheetham, A. K.; Friščić, T. Rapid Room-Temperature Synthesis of Zeolitic Imidazolate Frameworks by Using Mechanochemistry. *Angew. Chem., Int. Ed.* **2010**, 49 (50), 9640–9643.
- (27) Gao, W.-Y.; Sur, A.; Wang, C.-H.; Lorzing, G. R.; Antonio, A. M.; Taggart, G. A.; Ezazi, A. A.; Bhuvanesh, N.; Bloch, E. D.; Powers, D. C. Atomically Precise Crystalline Materials Based on Kinetically Inert Metal Ions via Reticular Mechanopolymerization. *Angew. Chem., Int. Ed.* **2020**, *59* (27), 10878–10883.
- (28) Karadeniz, B.; Howarth, A. J.; Stolar, T.; Islamoglu, T.; Dejanović, I.; Tireli, M.; Wasson, M. C.; Moon, S.-Y.; Farha, O. K.; Friščić, T.; Užarević, K. Benign by Design: Green and Scalable Synthesis of Zirconium UiO-Metal—Organic Frameworks by Water-Assisted Mechanochemistry. ACS Sustainable Chem. Eng. 2018, 6 (11), 15841—15849.
- (29) Užarević, K.; Wang, T. C.; Moon, S.-Y.; Fidelli, A. M.; Hupp, J. T.; Farha, O. K.; Friščić, T. Mechanochemical and solvent-free assembly of zirconium-based metal—organic frameworks. *Chem. Commun.* **2016**, *52*, 2133—2136.
- (30) Karadeniz, B.; Žilić, D.; Huskić, I.; Germann, L. S.; Fidelli, A. M.; Muratović, S.; Lončarić, I.; Etter, M.; Dinnebier, R. E.; Barišić, D.; Cindro, N.; Islamoglu, T.; Farha, O. K.; Friščić, T.; Užarević, K. Controlling the Polymorphism and Topology Transformation in Porphyrinic Zirconium Metal—Organic Frameworks via Mechanochemistry. *J. Am. Chem. Soc.* **2019**, *141* (49), 19214–19220.
- (31) Julien, P. A.; Užarević, K.; Katsenis, A. D.; Kimber, S. A. J.; Wang, T.; Farha, O. K.; Zhang, Y.; Casaban, J.; Germann, L. S.; Etter, M.; Dinnebier, R. E.; James, S. L.; Halasz, I.; Friščić, T. *In Situ* Monitoring and Mechanism of the Mechanochemical Formation of a Microporous MOF-74 Framework. *J. Am. Chem. Soc.* **2016**, *138* (9), 2929–2932.
- (32) Abrahams, B. F.; Hudson, T. A.; McCormick, L. J.; Robson, R. Coordination Polymers of 2,5-Dihydroxybenzoquinone and Chloranilic Acid with the (10,3)-*a* Topology. *Cryst. Growth Des.* **2011**, *11* (7), 2717–2720.
- (33) Nielson, K. V.; Zhang, L.; Zhang, Q.; Liu, T. L. A Strategic High Yield Synthesis of 2,5-Dihydroxy-1,4-benzoquinone Based MOFs. *Inorg. Chem.* **2019**, *58* (16), 10756–10760.
- (34) Morikawa, S.; Yamada, T.; Kitagawa, H. Crystal Structure and Proton Conductivity of a One-dimensional Coordination Polymer, {Mn(DHBQ)(H₂O)₂}. *Chem. Lett.* **2009**, 38 (7), 654–655.
- (35) Yamada, T.; Morikawa, S.; Kitagawa, H. Structures and Proton Conductivity of One-Dimensional M(dhbq)·nH2O (M = Mg, Mn, Co, Ni, and Zn, H2(dhbq) = 2,5-Dihydroxy-1,4-benzoquinone) Promoted by Connected Hydrogen-Bond Networks with Absorbed Water. *Bull. Chem. Soc. Jpn.* **2010**, 83, 42–48.
- (36) Dong, H.; Gao, H.; Geng, J.; Hou, X.; Gao, S.; Wang, S.; Chou, S. Quinone-Based Conducting Three-Dimensional Metal—Organic Framework as a Cathode Material for Lithium-Ion Batteries. *J. Phys. Chem. C* **2021**, *125* (38), 20814—20820.
- (37) Atzori, M.; Artizzu, F.; Sessini, E.; Marchio, L.; Loche, D.; Serpe, A.; Deplano, P.; Concas, G.; Pop, F.; Avarvari, N.; Mercuri, M. L. Halogen-bonding in a new family of tris(haloanilato)metallate(III) magnetic molecular building blocks. *Dalton Trans.* **2014**, *43*, 7006–7019.
- (38) Hmadeh, M.; Lu, Z.; Liu, Z.; Gándara, F.; Furukawa, H.; Wan, S.; Augustyn, V.; Chang, R.; Liao, L.; Zhou, F.; Perre, E.; Ozolins, V.; Suenaga, K.; Duan, X.; Dunn, B.; Yamamto, Y.; Terasaki, O.; Yaghi, O. M. New Porous Crystals of Extended Metal-Catecholates. *Chem. Mater.* **2012**, 24 (18), 3511–3513.